Cell Reports, Volume *32*

Supplemental Information

Enteric Glia Modulate Macrophage Phenotype and Visceral Sensitivity following Inflammation

Vladimir Grubišić, Jonathon L. McClain, David E. Fried, Iveta Grants, Pradeep Rajasekhar, Eva Csizmadia, Olujimi A. Ajijola, Ralph E. Watson, Daniel P. Poole, Simon C. Robson, Fievos L. Christofi, and Brian D. Gulbransen

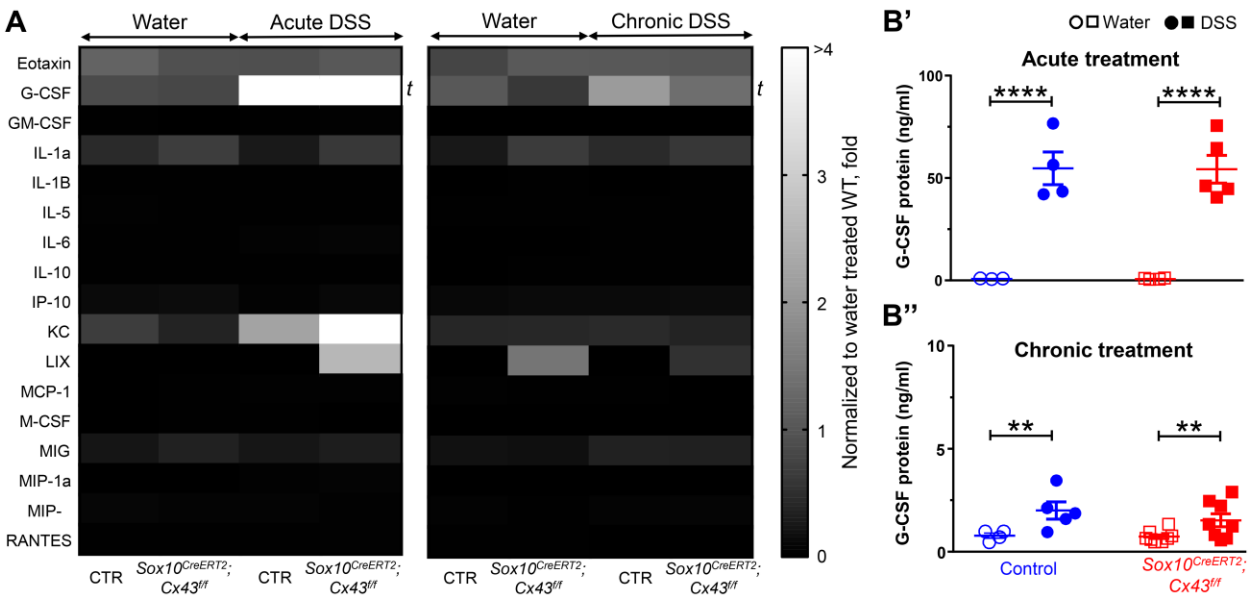

Figure S1 (*related to Fig 3A-B*)**. Intestinal inflammation-induced increase in serum concentration of G-CSF is not affected by the ablation of glial Cx43.** A heat map of relative protein concentration in mouse sera (**A**) after acute (left) or chronic (right) inflammation. 2-way ANOVA ($P < 0.05$): *t*, *treatment*. Note that the ablation of glial Cx43 did not further influence the inflammation-induced expression of G-CSF (**B**). **, $P = 0.002$; ****, $P < 0.0001$; 2-way ANOVA. N = 3-5 and 4-8 mice for acute and chronic DSS, respectively.

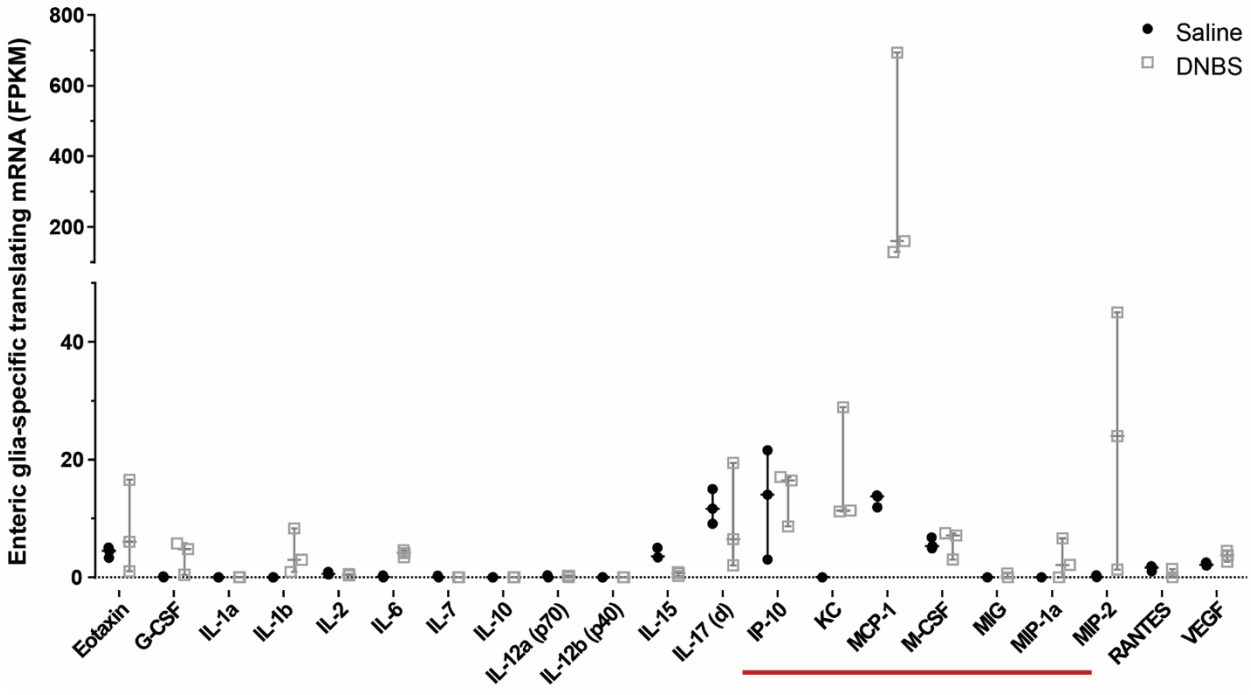

Figure S2 (*related to Fig 3A*)**. Enteric glia-specific expression of cytokine/chemokine transcripts.** The data are sourced from the published raw data set (Delvalle et al., 2018) where mice with a tamoxifen-sensitive targeted mutation of the ribosomal protein L22 (Rpl22) in enteric glia (Sox10::CreER$^{T2+/-}$/Rpl22$^{tm1.1Psam/}$J mice) were treated with an enema of 2,4-di-nitrobenzene sulfonic acid (DNBS) or saline. Tagged glia-specific ribosomes were extracted from colon tissue homogenates and transcript expression levels were reported as fragments per kilobase of transcript per million mapped reads (FPKM). Data shown as individual values and median ± 95% confidence interval (N = 3 mice). The red bar marks mediators affecting macrophage biology.

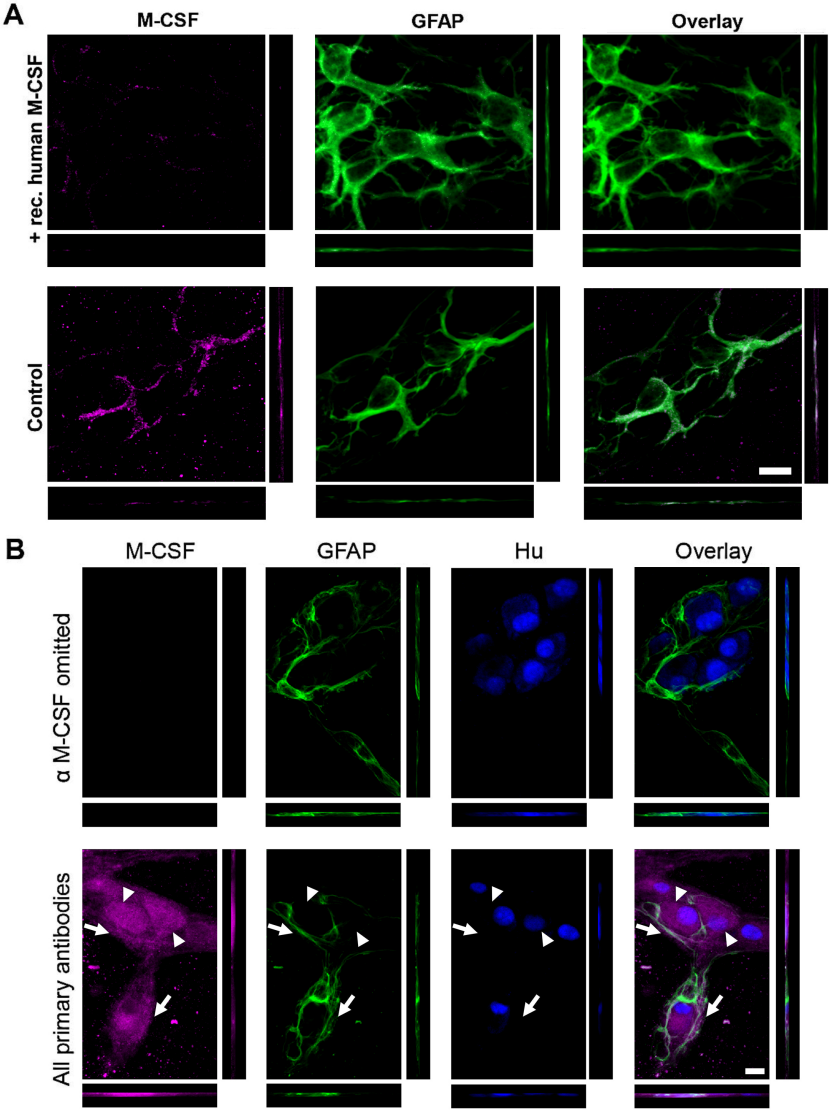

Figure S3 (*related to Figs 3C-F and 5D-G*)**. Characterization of the rabbit anti-M-CSF antibody.** Confocal images of whole-mount preparations from myenteric plexus of the mouse colon (A) and submucosal plexus of the human jejunum (B) labeled with antibodies against the glial fibrillary acidic protein (GFAP, green), M-CSF (magenta) and HuC/D (blue). Overlay images are on the far right. **A)** Preparations stained with the antibody mix pre-incubated with the recombinant human M-CSF protein (top) do not have the M-CSF immunoreactivity in comparison to the control preparations (bottom). **B)** The omission of the anti-M-CSF antibody (top) shows a lack of non-specific labeling of secondary antibodies. Arrows and arrowheads point to glia and neurons, respectively. Scale bars, 10 μm.

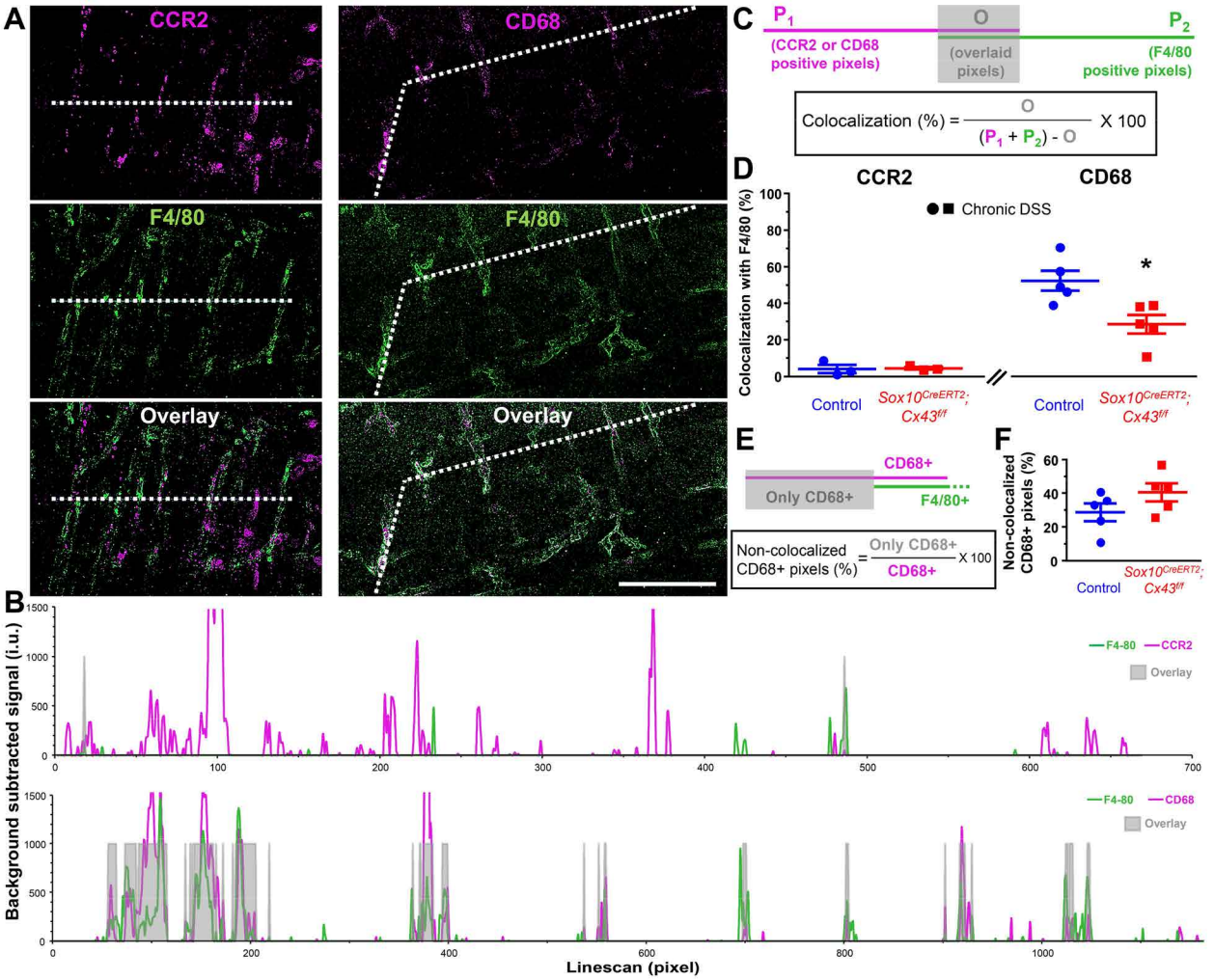

Figure S4 (*related to Fig 4D-E*)**. Co-localization of F4/80 immunoreactivity with CCR2 and CD68.** Using MetaMorph software we applied the Kirsch filter to all images to enhance edge detection and used linescans to quantify colocalization. **A)** Representative images after the Kirsch filtering showing markers of newly recruited macrophages (CCR2) or phagocytic macrophage phenotype (CD68) (top row), tissue-resident macrophages (F4/80) (middle row), and their overlays (bottom row). Dotted lines indicate linescans (shown in B). Scale bar, 100 um. **B)** Linescans of F4/80 immunoreactivity together with either CCR2 (top) or CD68 (bottom) after the background subtraction. Overlayed signals are shaded with gray boxes. **C)** Analysis of colocalization. Schematic (top) depicts an overlay of two signals and defines the symbols used in the formula (bottom) to calculate colocalization. Positive pixels were defined as pixels with intensity above 3 SD above the average background. **D)** Colocalization of F4/80 positive pixels with either CCR2 (left) or CD68 (right) from whole-mount longitudinal muscle-myenteric plexus preparations of control (blue) and *Sox10^{CreERT2};Cx43$^{f/f}$* mice (red) after chronic DSS treatment. N = 3 to 5 mice. Data are shown as mean ± SEM. *, P = 0.0124, Welch's t-test. **E)** Analysis of CD68 labeling that was not colocalized to F4/80 signal. Schematic (top) depicts an overlay of two signals and defines the symbols used in the formula (bottom) to quantify non-colocalized CD68+ pixels (positive pixels were defined as above). **F)** CD68 labeling that was not colocalized to F4/80 signal was comparable between the control (blue) and *Sox10^{CreERT2};Cx43$^{f/f}$* (red) whole-mount longitudinal muscle-myenteric plexus preparations after chronic DSS treatment. N = 5 mice per group. Data are shown as mean ± SEM. *, P = 0.0124, Welch's t-test.

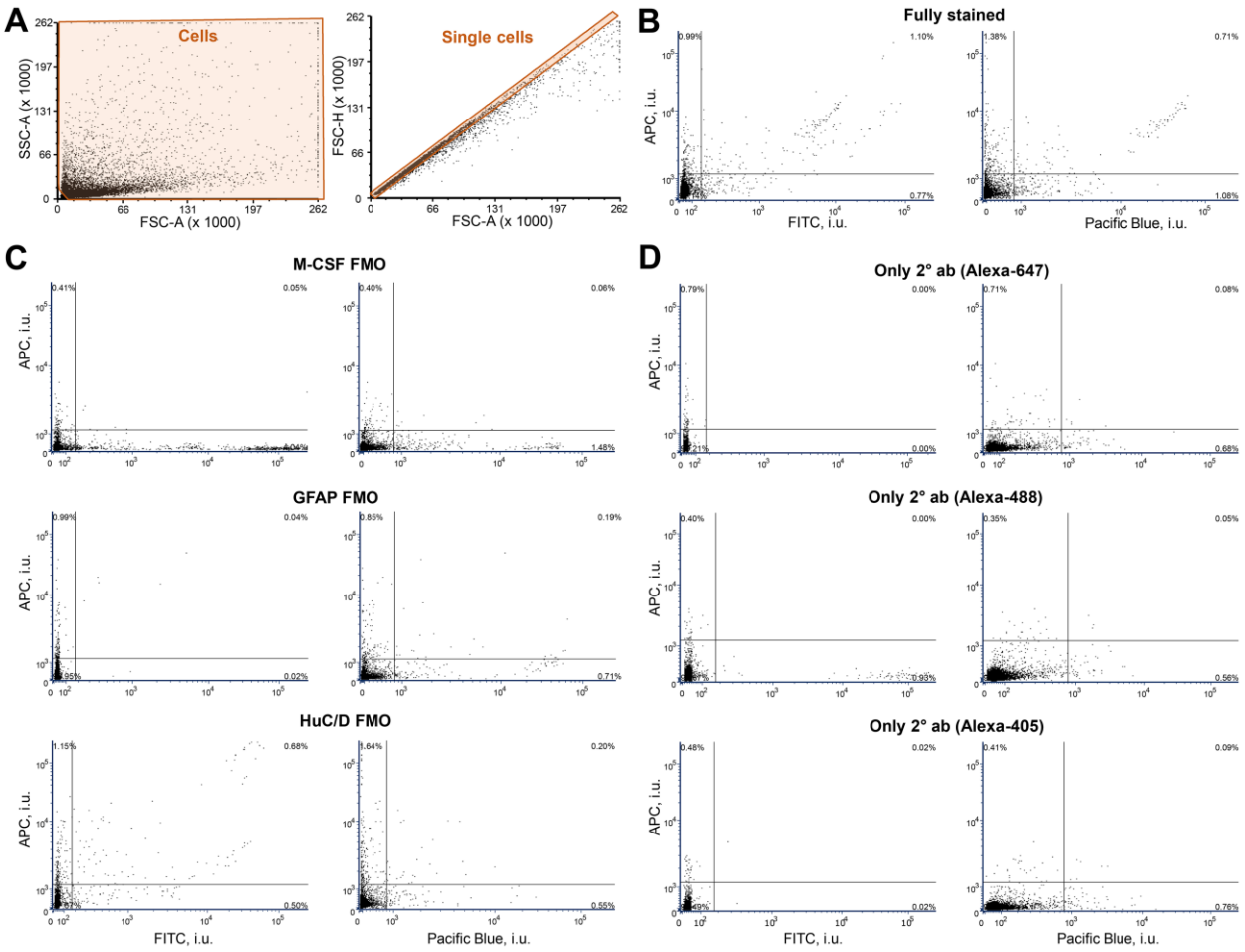

Fig S5 (*related to Fig 5A-E*)**. Gating and controls for flow cytometry. A)** Gating strategy to include single cells in flow cytometry analysis of cells dissociated from the muscular layer of mouse colons. We selected a wide cell population on the forward scatter (FSC) vs side scatter (SSC) plot (left) and then selected single events on the FSC area vs height (right). **B)** Fully stained sample. **C-D)** We used two sets of controls. A complementary pair of primary and secondary antibodies were omitted in the fluorescence minus one (FMO) controls (**C**), while only each of the secondary antibodies was used to stain the only secondary antibody (2° ab) controls (**D**). Each row shows complementary controls.

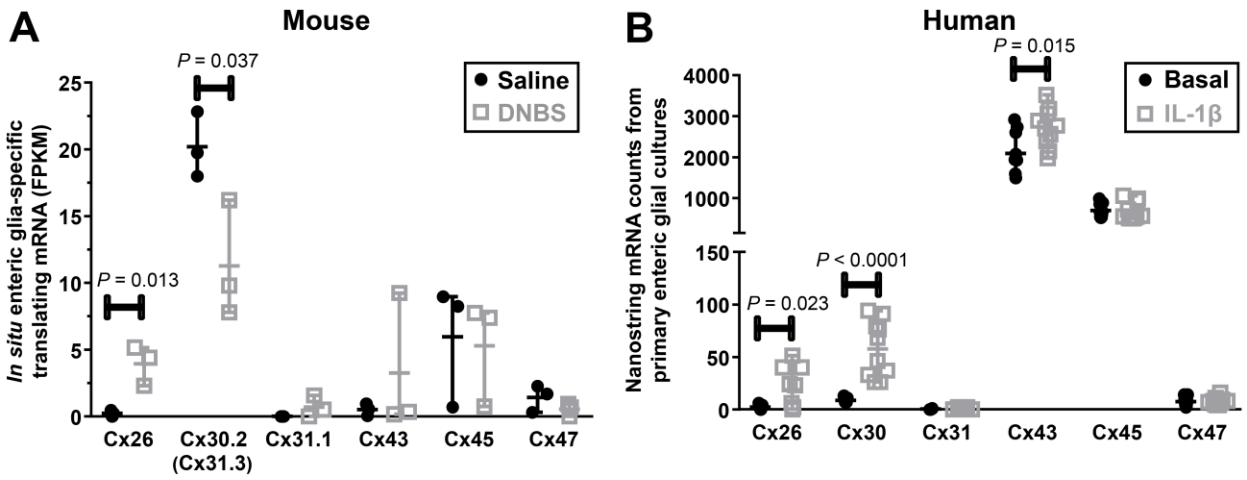

Figure S6 (*related to Fig 6 and Discussion*)**. Acute inflammation changes the expression of connexin genes in mouse and human enteric glia. A)** Mouse enteric glia *in situ* express different connexin isoforms after acute DNBS colitis. The data are sourced from the published raw data set (Delvalle et al., 2018) as described above (Fig S2). **B)** Expression of mRNA levels for connexins in human enteric glia in primary culture. Cx26, Cx30, Cx31, Cx43, Cx45, and C47 are expressed in hEGCs. Up-regulation occurred in Cx26, Cx30, and Cx43 with a 24 h IL1β induction. Analysis performed by nanostring. N = 3 mice (**A**) and 9 to 10 primary cultures of human enteric glia (**B**). Data shown as individual values and mean ± range. Statistical analysis performed by multiple *t*-tests.

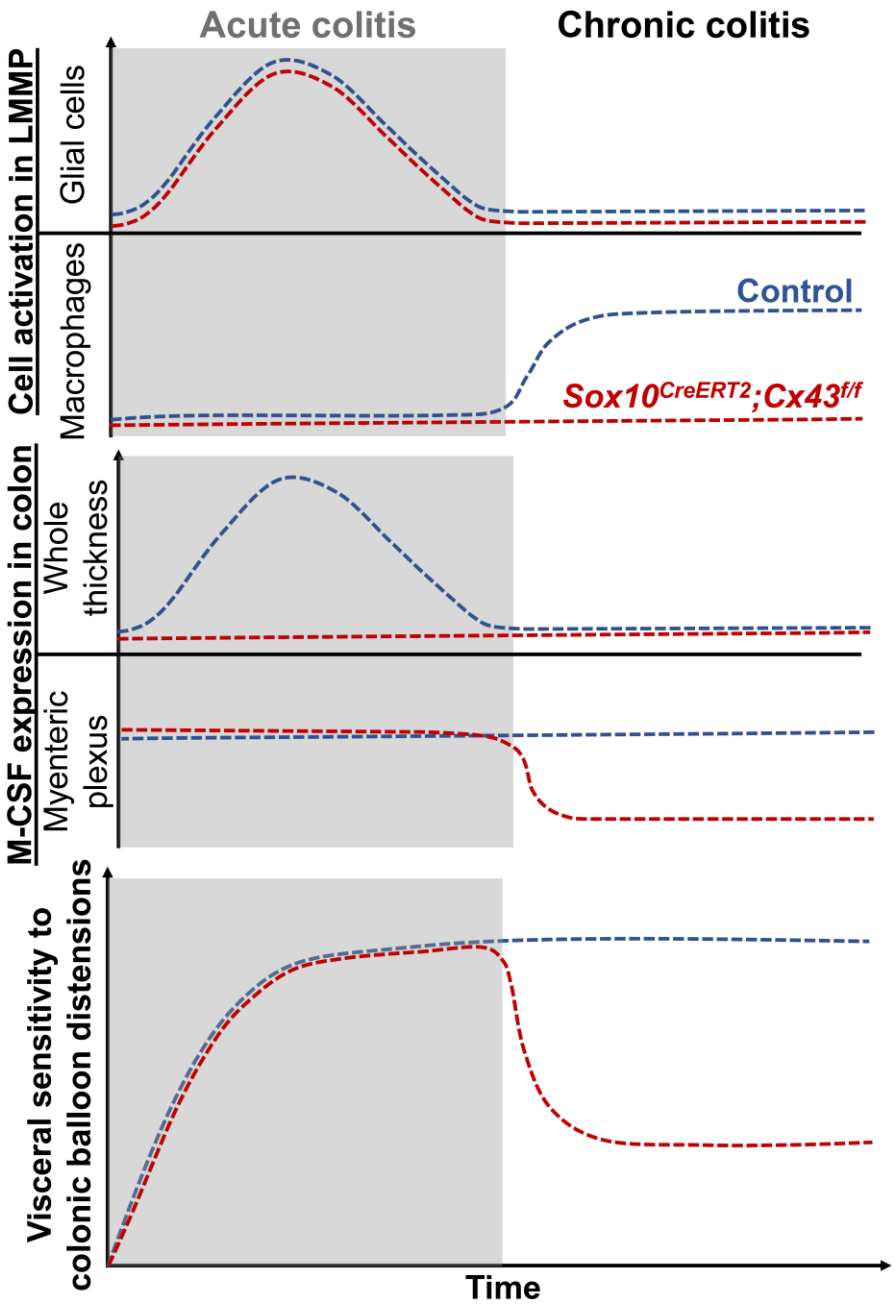

Figure S7 (*related to Figs 4C, 3B, 3F, 2D, and Discussion*)**. Temporal changes in an animal model of glia-specific knockout of Cx43.** Glial Cx43 is required for the global colonic production of M-CSF in acute intestinal inflammation. More importantly, in chronic colitis glial Cx43 mediates expression of M-CSF in the myenteric plexus, activation of muscularis macrophages, and chronic visceral sensitivity to colonic balloon distensions. The schematics are a summary of mouse data from Fig 2-4 and are not drawn to scale.

Table S1 (*related to Methods, IHC*)**. Primary and Secondary Antibodies Used.**

Antibody	Source	Catalog No.	Dilution
Primary Antibodies			
biotin mouse anti-HuC/D	Invitrogen, Carlsbad, CA	A21272	1:200
chicken anti-GFAP	Abcam, Cambridge, MA	ab4674	1:1,000
chicken anti-GFAP	Aves, Tigard, OR	GFAP87867983	1:2000
guinea pig anti-PGP9.5	Neuromics, Edina, MN	GP14104	1:500
rabbit anti-CCR2	Abcam, Cambridge, MA	ab216863	1:100
rabbit anti-M-CSF	Bioss, Woburn, MA	bs-4910R	1:100
rabbit anti-S100β	Abcam, Cambridge, MA	ab52642	1:200
rat anti-CD68, clone FA-11	AbD Serotec, Raleigh, NC	MCA1957	1:1,000
rat anti-F4/80	Abcam, Cambridge, MA	ab6640	1:100
rat anti-MHC class II	BioLegend, San Diego, CA	#107602	1:500
rat anti-MHC class II	Novus, Centennial, CO	NBP2-21789	1:200
Secondary Antibodies			
donkey anti-chicken Alexa 488	Jackson Immuno, West Grove, PA	703-545-155	1:500
donkey anti-rat Alexa 647	Jackson Immuno, West Grove, PA	712-605-150	1:500
donkey anti-rabbit Alexa 594	Jackson Immuno, West Grove, PA	711-585-152	1:400
donkey anti-guinea pig DyLight 405	Jackson Immuno, West Grove, PA	706-475-148	1:400
goat anti-chicken DyLight 405	Jackson Immuno, West Grove, PA	103-475-155	1:400
goat anti-chicken Alexa 488	Invitrogen, Carlsbad, CA	A-11039	1:400
goat anti-rabbit Alexa 488	Invitrogen, Carlsbad, CA	A-11034	1:400
goat anti-rat Alexa 594	Jackson Immuno, West Grove, PA	112-585-003	1:400
streptavidin DyLight 405	Jackson Immuno, West Grove, PA	016-470-084	1:400
streptavidin Alexa 594	Jackson Immuno, West Grove, PA	016-580-084	1:400

Table S2 (*related to Fig 1E-F*)**. Histological Disease Activity Scoring.**

Feature Scored	Score
epithelial damage	0-3
immune infiltration	0-3
crypt architecture	0-3
abscess present	Present (1) or absent (0)

0 = 0-5%, 1 = 6-25%, 2 = 26-50%, 3 = 51-100% of tissue affected.

Table S4 (*related to Methods section "RNA isolation from primary human enteric glia and NanoString nCounter Gene Expression Assay of selected connexins" and Fig S6B*)**. Nanostring Code set – listing the connexin genes, accession #s, and target sequences used for nanostring analysis and housekeeping genes used to normalize the data.**

	Accession	Target Sequence
Human connexins		
hCx26	NM_004004.5	GGCTGTCTGTTGTATTCATTGTGGTCATAGCACCTAACAACATTGTAGCCTC AATCGAGTGAGACAGACTAGAAGTTCCTAGTGATGGCTTATGATAGCA
hCx30	NM_006783.4	AGGCACGAAACCACTCGCAAGTTCAGGCGAGGAGAGAAGAGGAATGATTT CAAAGACATAGAGGACATTAAAAAGCAGAAGGTTCGGATAGAGGGGTCGC
hCx31	NM_001005752.1	GGTGGACCTACCTGTTCAGCCTCATCTTCAAGCTCATCATTGAGTTCCTCTT CCTCTACCTGCTGCACACTCTCTGGCATGGCTTCAATATGCCGCGCCT
hCx43	NM_000165.3	GCGAACCTACATCATCAGTATCCTCTTCAAGTCTATCTTTGAGGTGGCCTTC TTGCTGATCCAGTGGTACATCTATGGATTCAGCTTGAGTGCTGTTTAC
hCx45	NM_001080383.1	TTGCTGGCAAGGACCGTGTTTGAGGTGGGTTTTCTGATAGGGCAGTATTTT CTGTATGGCTTCCAAGTCCACCCGTTTTATGTGTGCAGCAGACTTCCTT
hCx47	NM_020435.2	GGAATGGGGCTCTGGGTTCCTGCCTGTGGCCTGTCTGTCCTCCTCCCTAAT TCAGACCCAGCCTCAAGAGGAAAGGGAGTAAAATAAAACTAACTTGTTT
Housekeeping genes		
ADA1	NM_053053.3	GCAGGTGCACAGGGAAGTCATCCCTACACATACTGTCTATGCTCTTAACATT GAAAGGATCATCACGAAACTCTGGCATCCAAATCATGAAGAGCTGCAG
CTNNB1	NM_001098210.1	TCTTGCCCTTTGTCCCGCAAATCATGCACCTTTGCGTGAGCAGGGTGCCAT TCCACGACTAGTTCAGTTGCTTGTTCGTGCACATCAGGATACCCAGCGC
NMNAT1	NM_022787.3	CCGAGAAGACTGAAGTGGTTCTCCTTGCTTGTGGTTCATTCAATCCCATCAC CAACATGCACCTCAGGTTGTTTGAGCTGGCCAAGGACTACATGAATGG
RBP1	NM_002899.3	TGATCATCCGCACGCTGAGCACTTTTAGGAACTACATCATGGACTTCCAGG TTGGGAAGGAGTTTGAGGAGGATCTGACAGGCATAGATGACCGCAAGTG

ADA1, adenosine deaminase 1; CTNNB1, human gene encoding β-catenin; NMNAT1, nicotinamide nucleotide adenylyltransferase 1; RBP1, retinol-binding protein 1.